Dielectric dispersions in pentakis methyl ammonium bismuthate single crystals. I. $(CH_3NH_3)_5Bi_2Br_{11}$

1992 J. Phys.: Condens. Matter 4 2687

(http://iopscience.iop.org/0953-8984/4/10/029)

J. Phys.: Condens. Matter 4 (1992) 2687–2694. Printed in the UK

Dielectric dispersions in pentakis methyl ammonium bismuthate single crystals: I. $(CH_3NH_3)_5Bi_2Br_{11}$

Cz Pawlaczyk†, K Planta‡, Ch Bruch‡, J Stephan‡ and H-G Unruh‡

† Institute of Molecular Physics, Polish Academy of Sciences, Smoluchowskiego 17/19, PL-60179 Poznan, Poland

‡ Fachbereich Physik, Universität des Saarlandes, W-6600 Saarbrücken, Federal Republic of Germany

Received 13 September 1991

Abstract. The dielectric dispersion of the permittivity ε_c^* in $(CH_3NH_3)_5Bi_2Br_{11}$ single crystals has been studied in the frequency range from 1 MHz to 20 GHz between 60 and 400 K and from 18 to 40 GHz and from 60 to 90 GHz near room temperature. Two temperature-dependent relaxators contribute to the permittivity near the ferroelectric phase transition at $T_{c1} = 311.5$ K; a low-frequency relaxator in the megahertz region showing a critical slowing down and a high-frequency relaxator in the gigahertz region which is thermally activated. Near the second phase transition at $T_{c2} = 77$ K a third, critically temperature-dependent contribution determines the dielectric properties of the crystal. The origin of the discovered contributions is discussed with respect to the structure of the crystal.

1. Introduction

Recently we have noticed interesting dynamic dielectric properties of the new ferroelectric $(CH_3NH_3)_5Bi_2Br_{11}$ (MAPBB) [1]. The crystal is orthorhombic at room temperature with a space group $Pca2_1$ and, at $T_{c1} = 311.5$ K, undergoes a phase transition to the paraelectric phase ($Pcab$), which is accompanied by a considerable low-frequency dielectric anomaly along the polar c direction. Our foregoing measurements of the dielectric dispersion near T_{c1} revealed an almost perfect Debye-type relaxation in the frequency range between 10 MHz and 1 GHz with a critical slowing down of the relaxation frequency $f_{\varepsilon 1}$. A distinct deviation from this behaviour was detected at frequencies above 1 GHz, which was particularly apparent at some distance from T_{c1} in both phases. It was noted that the dielectric spectra may be fitted by the sum of the contributions of two relaxators with the characteristic frequencies $f_{\varepsilon 1}$ and $f_{\varepsilon 2}$. We suggested that not only relaxator 1 but also relaxator 2 displays a critical dependence on temperature [1]. The Debye-like dispersion due to relaxator 1 and its critical slowing down at T_{c1} have been confirmed recently [2]. However, no further contribution to the dielectric dispersion has been mentioned there.

In this paper the above suggestions have been checked under improved experimental conditions compared with [1] and more precise measurements have been performed in a coaxial line up to 20 GHz. Furthermore, investigations in the microwave bands K, R and E have been added and the measurements in the coaxial line have been extended to low temperatures. Thus, measuring facilities enabled us to study the dynamic dielectric

0953-8984/92/102687 + 08 $04.50

behaviour of MAPBB near the low-temperature phase transition at $T_{c2} = 77$ K which is manifested as an anomaly on the static dielectric permittivity [1] and an increase in the spontaneous polarization below this temperature [3].

2. Experimental details

The measured MAPBB single crystals were obtained in the same manner as those described in [1]. For measurements in the coaxial line, cylindrical samples with the ferroelectric *c* axis parallel to the cylinder axis were used. Above room temperature, where the permittivity of MAPBB is relatively high, samples 2 mm in diameter and 1 mm in thickness were measured; for low-temperature measurements the corresponding dimensions of the samples were 5 mm and 1 mm, respectively.

In the waveguide measurements, rectangular samples were used which totally fill the cross section of the waveguides. Their dimensions were 10.668 mm × 4.318 mm (K band, 18–26.5 GHz), 7.112 mm × 3.556 mm (R band, 26.5–40 GHz) and 3.099 mm × 1.550 mm (E band, 60–90 GHz). In order to measure the dielectric properties the critical direction had to be parallel to the electric field vector of the propagating TE_{10} mode. Therefore, the samples were oriented with the ferroelectric *c* axis parallel to the smaller side of the waveguide. The sample thickness had to be chosen between an upper limit and lower limit, where the upper limit is given by the dynamic range of the receiver (about 60 dB), while the lower limit arises from the decreasing accuracy of the measured dielectric properties with decreasing thickness of the samples. Thus, the sample thickness was varied from 1.05 mm (E band) to 2.76 mm (K band). The samples were pasted into flanges by means of silver-filled epoxy paste of high conductivity.

In the frequency range from 1 MHz to 20 GHz we used a completely computer-controlled coaxial reflectometer. It is made up of an HP4191A impedance analyser (1 MHz–1 GHz) and an HP8510B network analyser with an HP8514B *S*-parameter test set (45 MHz–20 GHz) and an HP8350B sweep oscillator. Both analysers were connected to the sample holder by coaxial switches.

Two different sample holders were used, above and below room temperature, respectively. The cylindrical sample with its axis parallel to the critical direction formed a section of the radial transmission line terminating the coaxial line. The complex permittivity $\varepsilon^* = \varepsilon' - i\varepsilon''$ was calculated from the measured reflection coefficient.

The temperature control in the range from 290 to 400 K was achieved by an electric furnace and between 60 and 300 K by inserting the respective sample holder into a Leybold continuous-flow cryostat. The temperature was measured by platinum resistors Pt100 and stabilized to within ±0.01 K.

For the measurements above 18 GHz, three different bands of rectangular waveguides as mentioned above were used. Here, the complex dielectric permittivity was calculated from the ratio of the simultaneously determined complex transmission and reflection coefficients of the samples that were measured by a Scientific Atlanta 1753 series receiver using superheterodyne techniques.

The waveguide measurements were performed in a temperature range from 295 to 360 K using electric heating. The temperature was measured with platinum resistors and stabilized to within ±0.05 K. The absolute temperature accuracy for all the measurements was estimated at 1 K.

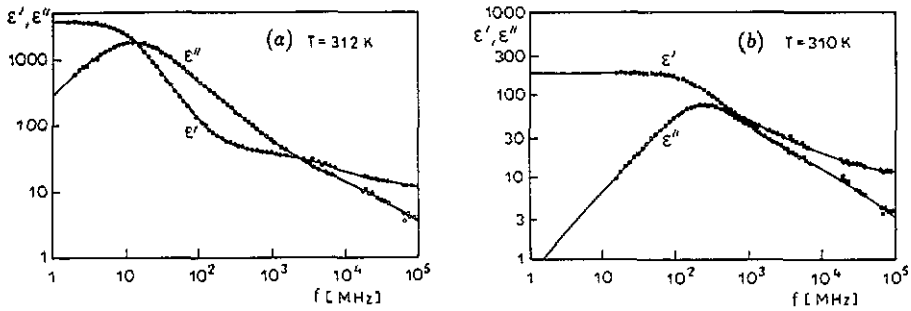

Figure 1. Dielectric spectra of an MAPBB sample at (a) 312 K and (b) 310 K. The full curves were obtained by fitting with equation (1); the fitting parameters were as follows: for (*a*), $A = 0.99$, $\Delta\varepsilon = 3746$, $\tau_{\varepsilon_1} = 1.25 \times 10^{-8}$ s, $\tau_{\varepsilon_2} = 3.63 \times 10^{-11}$ s, $h_1 = 0.021$ and $h_2 = 0.31$; for (*b*) $A = 0.80$, $\Delta\varepsilon = 180$, $\tau_{\varepsilon_1} = 6.47 \times 10^{-10}$ s, $\tau_{\varepsilon_2} = 4.42 \times 10^{-11}$ s, $h_1 = 0.0087$ and $h_2 = 0.29$.

3. Results

3.1. Dielectric behaviour near the ferroelectric phase transition at T_{cl}

As has already been shown [1], the dielectric spectra of MAPBB may be described as a sum of two relaxators 1 and 2 characterized by the relaxation times τ_{ε_1} and τ_{ε_2}:

$$\varepsilon^*(\omega) = \varepsilon_\infty + A\,\Delta\varepsilon/[1 + (i\omega\tau_{\varepsilon_1})^{1-h_1}] + (1 - A)\,\Delta\varepsilon/[1 + (i\omega\tau_{\varepsilon_2})^{1-h_2}]. \qquad (1)$$

The parameter A determines the part of the dispersion strength $\Delta\varepsilon$ that is related to relaxator 1.

The studies of MAPBB in the microwave bands K, R and E have confirmed the correctness of this proposition. Figure 1 displays the dielectric spectra of MAPBB at 312 and 310 K from the measurements in a coaxial line and in the microwave bands K, R and E. The full curves have been obtained by a least-squares fit of the data to equation (1). Note that the fitting was done simultaneously for log ε' and log ε'' in order to give comparable weights to both contributions. The fits show that equation (1) describes the experimental results very well and confirm the assumption that the permittivity of MAPBB consists essentially of the contributions of two independent relaxators.

Relaxators 1 and 2 differ fundamentally in their physical behaviours. The characteristic frequency f_{ε_1} of relaxator 1 shows a critical slowing down, whereas the frequency f_{ε_2} of relaxator 2 depends only weakly on temperature (figure 2). In order to determine its dependence on temperature exactly, measurements in a wider range of temperatures are necessary (see section 3.2). In [1] it has been suggested that relaxator 2 also shows a critical slowing down near T_{c1}. The results of the more accurate measurements shown in the present paper and fitted to a more appropriate logarithmic scale reveal that this suggestion was incorrect.

3.2. Properties of relaxator 2 below T_{cl}

The dielectric contribution of relaxator 1 of MAPBB diminishes promptly below T_{c1} (figure 3). At 300 K this contribution has decreased to 10% of the whole dispersion and far below this temperature it is possible to observe the contribution from relaxator 2

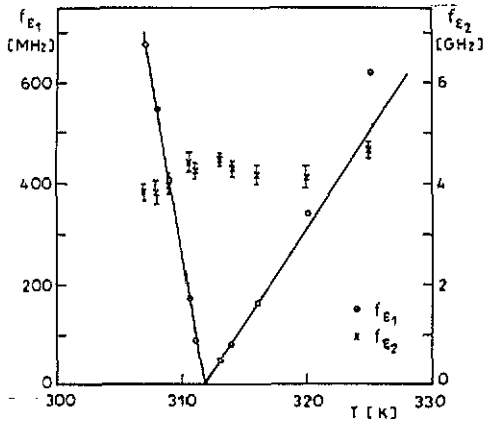

Figure 2. Temperature dependence of the relaxation frequencies f_{ε_1} and f_{ε_2} in the vicinity of T_{c1}.

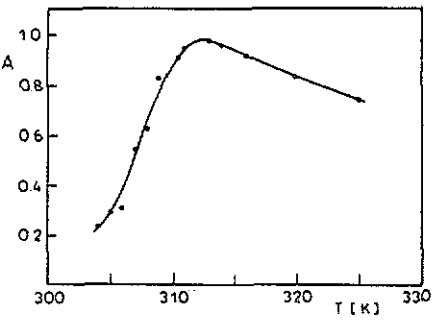

Figure 3. Temperature dependence of the coefficient A which determines the part of the dispersion strength $\Delta\varepsilon$ related to relaxator 1.

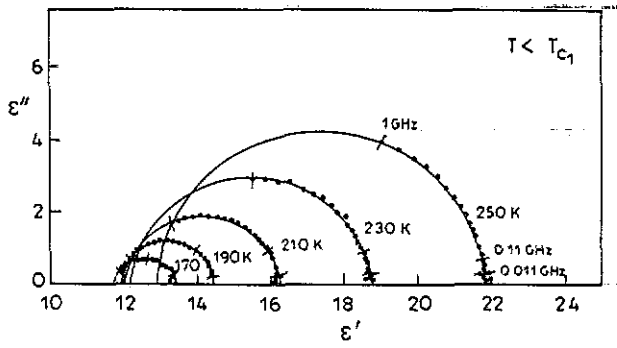

Figure 4. Dielectric dispersion of ε_c^* sufficiently far below T_{c1} where only relaxator 2 determines the dielectric dispersion.

separately and almost without the contribution from relaxator 1. In figure 4, Cole–Cole plots are presented for an MAPBB sample (diameter, 5 mm; $d = 1.00$ mm) at several temperatures sufficiently far below T_{c1}. The full curves were obtained by fitting the data to the Cole–Cole formula

$$\varepsilon^*(\omega) = \varepsilon_\infty + \Delta\varepsilon_2/[1 + (i\omega\tau_{\varepsilon_2})^{1-h_2}] \tag{2}$$

where the subscript 2 indicates that relaxator 2 is the postulated source of this contribution. This assumption is justified only at temperatures far enough below T_{c1}.

The relaxation time τ_{ε_2} depends on the temperature according to the Arrhenius law as displayed by figure 5:

$$\tau_{\varepsilon_2} = \tau_0 \exp(\Delta U/kT) \tag{3}$$

where ΔU is an activation energy, k the Boltzmann constant and τ_0 a constant. The activation energy has been evaluated by fitting equation (3) to the results presented in

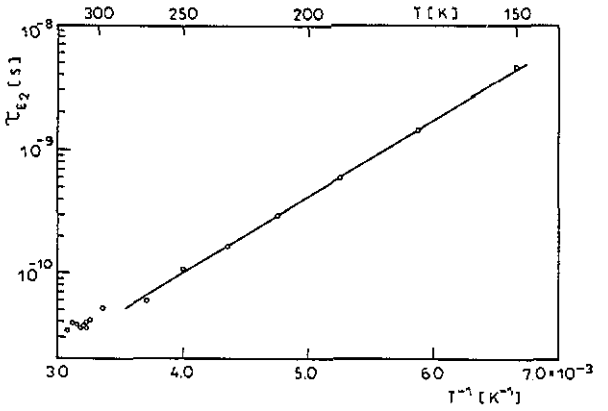

Figure 5. Arrhenius plot for the relaxation time τ_{ε_2} of relaxator 2.

figure 5, yielding $\Delta U = 0.12$ eV. Thus the origin of the contribution from relaxator 2, characterized by the relaxation time τ_{ε_2}, is a thermally activated process with an activation energy of 0.12 eV.

3.3. Dielectric behaviour near the low-temperature transition at T_{c2}

Studies of the dielectric dispersion in the neighbourhood of the low-temperature phase transition at $T_{c2} = 77$ K reveal a pronounced relaxation of a critical nature in the range between 1 MHz and 1 GHz. This is shown in figure 6, where Cole–Cole plots are presented for $T > T_{c2}$ and $T < T_{c2}$, and in figure 7, which presents the temperature dependences of ε_s, ε_∞ and $\Delta\varepsilon_3 = \varepsilon_s - \varepsilon_\infty$. In this temperature range the dielectric behaviour is also describable by the Cole–Cole formula with parameters $\Delta\varepsilon_3$, $f_{\varepsilon_3} = 1/2\pi\tau_{\varepsilon_3}$ and h_3. Above T_{c2}, $\Delta\varepsilon_3$ obeys the Curie–Weiss law whereas below T_{c2} it decreases faster than would be expected from the linear dependence of $1/\Delta\varepsilon_3(T)$ slightly below T_{c2}.

The temperature dependence of the relaxation frequency f_{ε_3} (figure 8) is of the critical-slowing-down type; however, the non-linear dependence of $f_{\varepsilon_3}(T)$ resembles the dependence known for ferroelectric crystals with diffuse phase transitions.

4. Discussion

The results of the measurements of the dynamic dielectric properties of MAPBB are summarized in figure 9. Close to T_{c1}, where the spectra are described by means of equation (1), two temperature-dependent contributions to the permittivity can be distinguished, contribution 1 with the strength $\Delta\varepsilon_1 = A\ \Delta\varepsilon$ and contribution 2 with the strength $\Delta\varepsilon_2 = (1 - A)\ \Delta\varepsilon$. The contribution from relaxator 1 exhibits a critical slowing down, while the strength $\Delta\varepsilon_1$ obeys the Curie–Weiss law. At temperatures $T < T_{c1}$, $\Delta\varepsilon_1$ becomes small compared with $\Delta\varepsilon_2$. The relaxation time τ_{ε_2} of relaxator 2 depends on temperature according to the Arrhenius law, indicating a thermally activated process as its origin. In the vicinity of the second phase transition at $T_{c2} = 77$ K, the dielectric behaviour of MAPBB is determined by a contribution from relaxator 3 of strength $\Delta\varepsilon_3$ obeying again the Curie–Weiss law. Its relaxation frequency f_{ε_3} exhibits a critical slowing

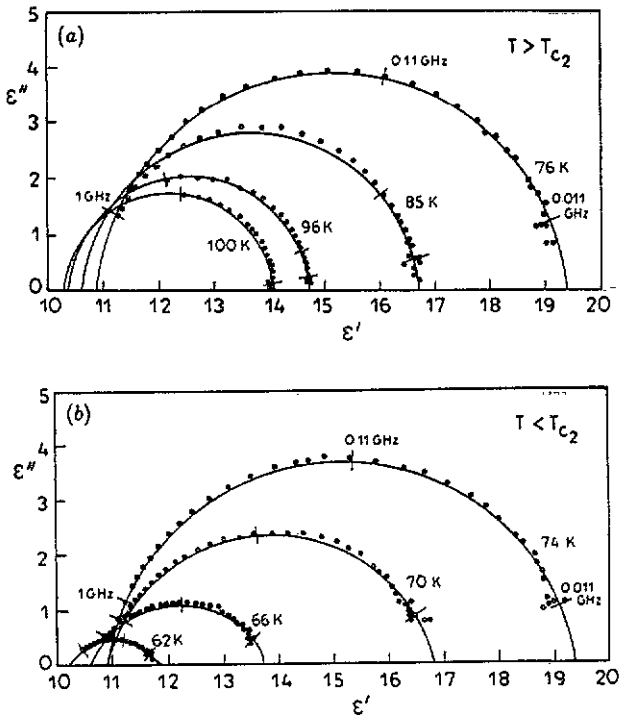

Figure 6. Dielectric dispersion of ε_c^* of MAPBB measured (a) above and (b) below the phase transition at T_{c2}. The full curves were obtained by fitting the data to the Cole–Cole formula (equation (2)) with parameters $\Delta\varepsilon_3$, τ_{ε_3} and h_3.

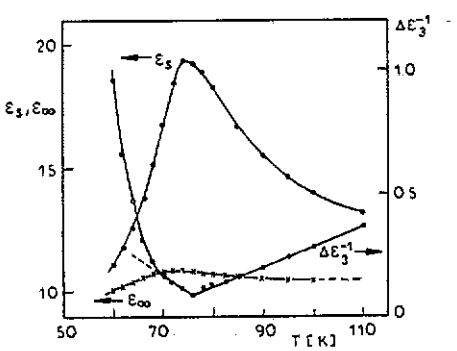

Figure 7. Temperature dependence of the parameters ε_s, ε_∞ and $\Delta\varepsilon_3 = \varepsilon_s - \varepsilon_\infty$ of relaxator 3.

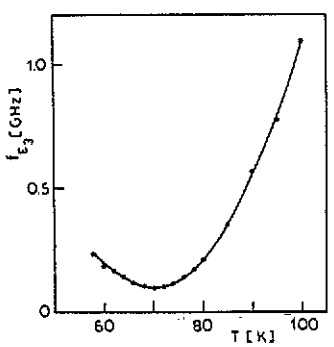

Figure 8. Temperature dependence of the relaxation frequency f_{ε_3} of relaxator 3.

down, too. It should be noticed that the values of ε near T_{c2} reported in the present paper are considerably lower than those of the static permittivity measured at audio frequencies [1, 3]. This is because in our dispersion measurements the mechanically clamped permittivity is determined, whereas at low frequencies the mechanically free permittivity is measured.

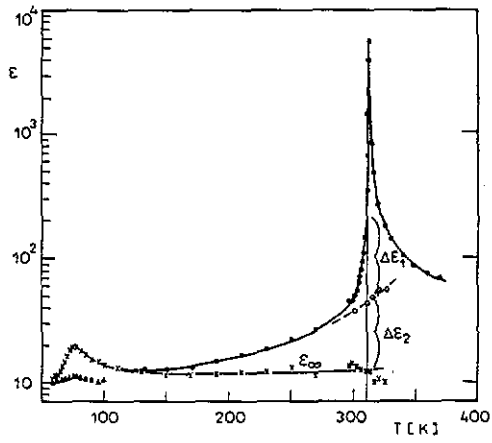

Figure 9. Temperature dependence of the various dielectric contributions to the permittivity of MAPBB in its crystallographic c direction. $\Delta\varepsilon_1 = A\ \Delta\varepsilon$ and $\Delta\varepsilon_2 = (1 - A)\ \Delta\varepsilon$ denote the strengths of relaxators 1 and 2, respectively.

In [1] we suggested that the reason for the phase transition at T_{c1} is an ordering–disordering process of the pair C(21)–N(21), C(22)–N(22) of methylammonium cations, where the labelling of the ions is taken from [4]. According to the results of the structural investigations [4] these cations are ordered at room temperature. However, new structural investigations [5] performed on the isomorphous compound $(CH_3NH_3)_5Bi_2Cl_{11}$ (MAPCB) both above (349 K) and below (294 K) the phase transition at $T_{c1} = 308$ K showed another arrangement of the cations; the pair C(i1)–N(i1) ($i = 1, 2$) is ordered whereas the pair C(i2)–N(i2) is disordered in both phases and all these cations cannot be involved in this phase transition.

On the other hand, differences of the ordering above and below T_{c1} were found [5] for C(3)–N(3) cations which are located in the middle of each edge of the orthorhombic unit cell. It has been assumed [5] that the phase transition at T_{c1} is brought about by the ordering–disordering process of this cation. Thus the observed contribution of relaxator 1 displaying critical properties in MAPBB may be interpreted as the response of the interacting C(3)–N(3) cations. The other pair of C(i2)–N(i2) cations ($i = 1, 2$) is assumed to be disordered in both phases as in the case of MAPCB. The disorder is based on two equilibrium positions of each C(i2)–N(i2) cation, which are occupied with distinct probabilities [5]. Therefore, thermally activated motions of the C(i2)–N(i2) cations jumping from one position to the other may be the source of the contribution from relaxator 2, which is characterized by the Arrhenius-type temperature dependence of the relaxation frequency f_{ε_2}. The energy barrier between the physically different equilibrium positions is given by the activation energy of 0.12 eV found in the present dielectric studies. Finally, the critical contribution of relaxator 3 revealed near T_{c2} indicates that a cooperative ordering interaction in the crystal exists. Because of the lack of structural data near T_{c2} it is hard to draw any conclusions about the molecular origin of this contribution.

Acknowledgment

The authors thank the Deutscher Akademischer Austauschdienst for the support of one of us (CzP) which enabled this joint work to be carried out.

References

[1] Pawlaczyk Cz, Motsch H, Jakubas R and Unruh H-G 1990 *Ferroelectrics* **108** 127
[2] Iwata M and Ishibashi Y 1990 *J. Phys. Soc. Japan* **59** 4239
[3] Mroz J and Jakubas R 1989 *Solid State Commun.* **72** 813
[4] Matuszewski J, Jakubas R, Sobczyk L and Glowiak T 1990 *Acta Crystallogr.* C **46** 1385
[5] Lefebvre J, Carpentier P and Jakubas R 1991 *Acta Crystallogr.* B **47** 228